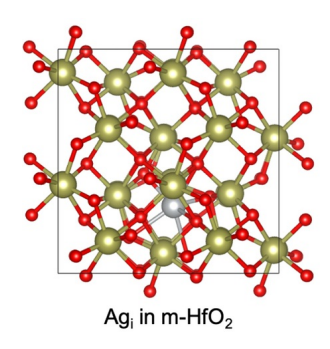
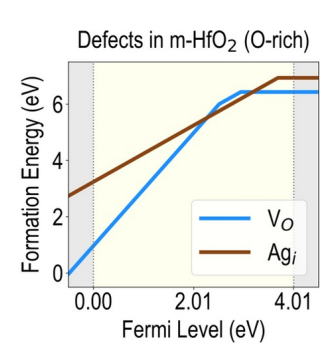
## Metadata of the article that will be visualized in OnlineFirst

ArticleTitle	Role of defects in re-	sistive switching dynamics of memristors	
Article Sub-Title			
Article Copy Right	The Author(s), under exclusive licence to The Materials Research Society (This will be the copyright line in the final PDF)		
Journal Name	MRS Communications		
Corresponding Author	FamilyName	Tutuncuoglu	
	Particle		
	Given Name	Gozde	
	Suffix		
	Division	Electrical and Computer Engineering Department	
	Organization	Wayne State University	
	Address	5050 Anthony Wayne Drive, Detroit, MI, 48202, USA	
	Phone		
	Fax		
	Email	gozde@wayne.edu	
	URL		
	ORCID	http://orcid.org/0000-0001-8812-5999	
Author	FamilyName	Mannodi-Kanakkithodi	
	Particle		
	Given Name	Arun	
	Suffix		
	Division	School of Materials Engineering	
	Organization	Purdue University	
	Address	701 W Stadium Ave, West Lafayette, IN, 47907, USA	
	Phone		
	Fax		
	Email	amannodi@purdue.edu	
	URL		
	ORCID		
Schedule	Received	22 May 2022	
	Revised		
	Accepted	16 Aug 2022	

Abstract

Resistive-switching memristors are promising device structures for future memory and neuromorphic computing applications. Defects are shown to be critical for the conducting filament formation, and resulting device performance metrics of memristors. In this prospective article, we investigate the role of defects in the resistive-switching dynamics of filamentary-type memristors, and explore defect-engineering as an effective method to rationally design controllable conduction pathways. Specifically, we propose a data-centric approach that combines the defect-knowledge obtained from first principles calculations with the materials engineering and characterization efforts. *Graphical abstract:* 





Keywords (separated by '- Defects - Computation/computing - Oxide - Neuromorphic ')

Footnote Information



#### Early Career Materials Researcher Prospective



### Role of defects in resistive switching dynamics of memristors

Gozde Tutuncuoglu 🗓, Electrical and Computer Engineering Department, Wayne State University, 5050 Anthony Wayne Drive, Detroit, MI 48202, USA Arun Mannodi-Kanakkithodi, School of Materials Engineering, Purdue University, 701 W Stadium Ave, West Lafayette, IN 47907, USA

Address all correspondence to Gozde Tutuncuoglu at gozde@wayne.edu

(Received 22 May 2022; accepted 16 August 2022)

#### Abstract

Resistive-switching memristors are promising device structures for future memory and neuromorphic computing applications. Defects are shown to be critical for the conducting filament formation, and resulting device performance metrics of memristors. In this prospective article, we investigate the role of defects in the resistive-switching dynamics of filamentary-type memristors, and explore defect-engineering as an effective method to rationally design controllable conduction pathways. Specifically, we propose a data-centric approach that combines the defect-knowledge obtained from first principles calculations with the materials engineering and characterization efforts.

#### Introduction

Next-generation computing devices will require significant improvements in processing speed and energy efficiency. Until recently, the constant push towards higher performance computers has been fueled by a series of progressive efforts in Si-based CMOS technology. These efforts, driven by Moore's law,[1] focus primarily on miniaturization of device components, along with the introduction of novel materials (i.e., high-k dielectrics), and device architecture innovations. However, increasing power dissipation levels hinder this progress towards higher processing speeds. Additionally, the latency and the energy cost of data transfer between the processing and memory units of conventional von-Neumann based computation architectures imposes fundamental limits in the computation efficiency. [2] Neuromorphic computing addresses these shortcomings by mimicking the brain to perform highly parallel, compact and energy-efficient computations. [3,4] Resistiveswitching memristor devices stand as a promising enabler technology for neuromorphic computing paradigm, as they can emulate synaptic functionalities through their resistive-switching dynamics, and function as non-volatile memory units.

Memristor devices<sup>[5–7]</sup> are typically two-terminal systems, consisting of two metal electrodes (MEs) and an intermediate switching layer. These devices demonstrate voltage-history dependent resistance levels as a result of various stoichiometric, structural and compositional changes in response to an electric field. [8,9] Due to their promising device metrics and early demonstrations of synaptic functionalities, a significant research effort is directed to a special class of memristor devices called the filamentary-type memristors, for which, stoichiometric, structural or compositional changes intensify in the spatially confined nanoscale filament geometry. Since these filaments effectively serve as conduction pathways, memristor resistance levels strongly change as a function of the physical properties of the conductive filaments (CF).[10–12]

Efficient deployment of filamentary-type memristor technology in neuromorphic computing requires high ON/OFF resistance ratios, multi-level resistance states, symmetric and linear potentiation/depression, along with satisfactory retention and endurance characteristics. Despite encouraging results (i.e.,  $> 10^{12}$  cycles of endurance,  $> 10^6$  ON/OFF ratio, < 10 nm scalability, [13-15]) current state of the filamentary-type memristors fall short of the required device performance metrics for large scale adoption of the technology. Common issues include intra- and inter-device variability, limited number of controllable resistance states, and poor retention and endurance levels. [16,17] These shortcomings are often interlinked with the uncontrolled formation and evolution of CFs, [18,19] which are governed by the defect structures—i.e., imperfections in crystal lattice. Evidently, defect-engineering provides a promising pathway towards controlling the adverse effects of filament formation and evolution. In recent studies, reported in-situ characterization results confirm the role of defects in filament formation during memristor device operation, and rational introduction of defects is shown to enhance a number of device performance metrics.<sup>[20–22]</sup> In Fig. 1, we provide insitu characterization examples from the recent literature, that demonstrate the formation of CF within filamentary-type memristor device stack.

In this prospective article, we investigate the role of defects in the resistive-switching dynamics of filamentary-type memristors, and explore defect-engineering as an effective method to rationally design controllable conduction pathways. In order to achieve a comprehensive understanding of various defect structure formation dynamics and related electronic properties, we showcase first principles-based density functional theory (DFT) computations along with an overview of the literature. We also identify characterization techniques and defect-engineering approaches that can provide additional insights into the role of defects in resistiveswitching dynamics. We propose that theory, characterization and



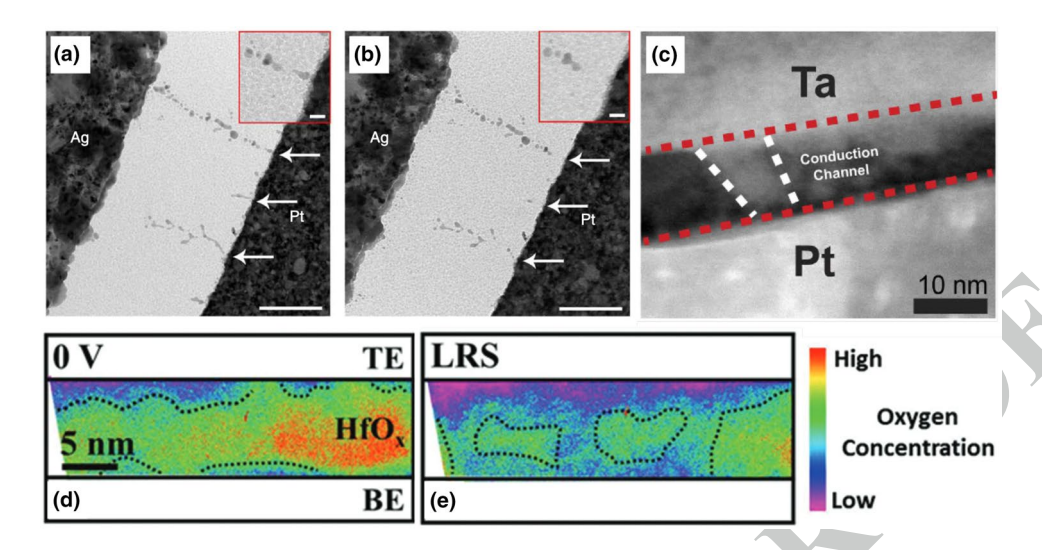


Figure 1. Ag CF formation (a) and dissolution (b) in Ag/SiO<sub>2</sub>/Pt memristor device. (Taken with permission from [23]) c) Formation of Ta-rich CF in Ta/HfO<sub>2</sub>/Pt memristor device. (Available via Creative Commons Attribution 4.0 from  $^{[24]}$ )  $V_O$  concentration maps at 0V bias (d), and Low-Resistance-State (LRS) (e), extracted from electron holography and TEM measurements in HfO<sub>x</sub> based memristors (Taken with permission from[20]).

defect-engineering are three integral components of an integrated strategy for unlocking an unprecedented level of control on memristor resistive-switching dynamics - a critical requirement for the large-scale adoption of this technology in memory and novel computing applications.

This paper is structured as follows. In Section II, we provide an overview of the computational methods we have employed for the calculations we present in this study. In Section III, we briefly introduce filamentary type memristors and describe their working principles.

Following this overview, Section IV focuses on the role of major defects on switching dynamics of anion-type and cationtype memristors, with a particular focus on  $V_0$  and metal cation defects. The paper concludes with a discussion on opportunities and challenges associated with exploring defect-engineering for superior device performance.

#### Methods

All DFT computations were performed using the Vienna Ab initio Simulation Package (VASP), [25] applying the generalized gradient approximation (GGA) parametrized by Perdew, Burke and Ernzerhof (PBE)[26] and using the projector-augmented wave (PAW) pseudopotentials.<sup>[27]</sup> The plane wave energy cutoff was set at 500 eV and all atomic structures were fully relaxed until forces on all atoms were less than 0.05 eV/Å. Brillouin zone integration was performed using a 3×3×3 Monkhorst-Pack k-point mesh for all oxides, including initial geometry optimization and defect calculations. Point defects are simulated by removing an (O) atom from the supercell to create a vacancy,  $V_O$ , and adding an (Ag) atom in the supercell to create interstitials,  $Ag_i$ . Defect formation energies are calculated for  $V_O$  and Ag<sub>i</sub> as a function of chemical potential  $\mu$ , charge q, and Fermi level  $E_F$ , using the following equations, written for HfO<sub>2</sub> as an example:

$$E^{F}(V_{O}) = E(HfO_{2} \text{ with } V_{O}) - E(HfO_{2}) + \mu_{O} + q * (E_{F} + E_{VBM})$$
(1)

$$E^{F}(Ag_{i}) = E(HfO_{2} \text{ with } Ag_{i}) - E(HfO_{2}) - \mu_{A}g + q * (E_{F} + E_{VBM})$$
(2)

On the right hand side, the first two terms are respectively the total DFT energies of the defect containing and bulk supercells,  $\mu$  is the chemical potential of the species involved in creating the defect, and  $E_{VBM}$  is the valence band maximum (VBM) of the oxide read from a separate calculation. Constraints are placed on the chemical potentials of all species, so as to ensure thermodynamic equilibrium conditions for the oxide and avoid the likelihood of decomposition to elemental standard states and/or other phases like Ag<sub>2</sub>O. These conditions can be written for m-HfO<sub>2</sub> as:

$$\Delta \mu_{\rm Hf} + 2 * \Delta \mu_{\rm O} = \Delta H(m - HfO_2) \tag{3}$$

$$2 * \Delta \mu_{Ag} + 2 * \Delta \mu_{O} < \Delta H(Ag_{2}O)$$
 (4)

$$\Delta \mu_{Hf} + 2 * \Delta \mu_{O} < \Delta H \text{ (other HfO}_2 \text{ phases)}$$
 (5)

Here,  $\Delta H(m-HfO_2) = E(m-HfO_2) - E(Hf) - 2 * E(O)$ . E(system) refers to the total DFT energy of the corresponding system. The chemical potentials of Hf, O, and Ag are referenced to their respective elemental standard states; e.g.,  $\mu_{\rm Hf} = \Delta \mu_{\rm Hf} + E({\rm Hf})$ , where E(Hf) is the DFT energy per atom of the elemental standard of Hf. Based on the above constraints, we select two types of chemical potential conditions: Hf-rich, when  $\Delta \mu_{\rm Hf} = 0 \, eV$ , and O-rich, when  $\Delta \mu_{\rm O} = 0 \, eV$ . Thus, defect formation energies are calculated at two extreme chemical growth conditions corresponding to excess metal and excess O respectively.

#### Filamentary switching mechanisms

Filamentary switching mechanisms are primary processes in memristors that govern device performance metrics. Switching behaviour in filamentary-type memristors span over two extreme non-volatile resistance levels as a result of the CF formation and rupture. These levels are called high resistance (HRS) and low resistance states (LRS), and represent 0 (off) and 1 (on) values of a potential binary logic operation. Filamentary-type memristors usually function in a bipolar fashion, switching on and off at opposite voltage polarities. Minimum applied voltage values that would drive this binary operation are referred as  $V_{\text{SET}}$  and  $V_{\text{RESET}}$ . If device resistance can be modified in a gradual manner, memristors can also function beyond the binary logic operation. This multi-level operation can be achieved through gradual modifications in the CF features (i.e., structure, geometry or length) via applied voltage pulses with controlled amplitude, duration and polarity. [28, <sup>29]</sup> Evolution of the CF, which is critical for optimum device operation, is driven through ion dynamics that respond to the electric-field (coupled with Joule heating in some cases). These dynamics have two special cases that can be classified according to the charged nature of the filament forming ions.

#### Anion migration

Anion migration, also known as valence charge mechanism (VCM), is driven by the transport of mobile anions/vacancies in response to the electric field between top and bottom electrodes of the memristor [(Fig. 2(a)]. Anion migration is usually the dominating switching mechanism in filamentary transitionmetal oxide (TMO) memristors, where oxygen anions drift in the opposite direction of the applied voltage, leaving  $V_0$ s

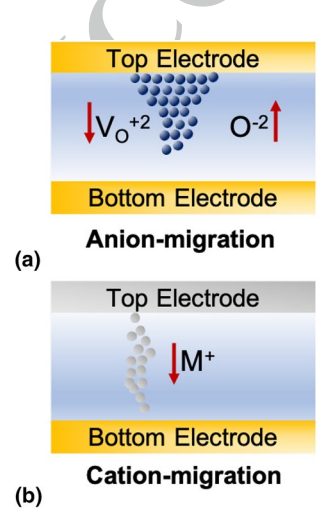


Figure 2. Anion and cation transport during resistive-switching process.

behind. Reported first-principles calculations, extensive characterization results, along with their voltage polarity responses, indicate that resistance-switching is driven by positively charged  $V_o$ s  $(V_o^{+2})$ , analogous to negatively charged oxygen anions  $(O^{-2})$  in filamentary TMO memristors. [30-32]

#### Cation migration

Cation migration, also known as electrochemical metallization mechanism (ECM), is based on the movement of electrochemically active metal cations through a solid electrolyte in response to the electric field. The oxidized mobile metal cations liberated from the electrochemically active ME (top electrode in Fig. 2(b), such as Ag and Cu, form CFs as a result of electrochemical redox reactions. These metallic filaments form a conductive bridge between the active and inert electrodes of the filamentary-type memristor. The mobility of the cations in the switching medium, governed by migration energy barrier  $(E_a)$ , and the rate of redox reactions are critical parameters that govern the device performance metrics.[33,34]

Anion and cation migration processes are governed by defect dynamics in switching layer of the filamentary-type memristor devices. The following section discusses the role of defects, and demonstrates how to model, characterize and engineer their impact on device performance metrics.

#### Role of defects in switching dynamics

Controlling and engineering defects significantly modify the electronic properties of semiconductor and insulator materials by disrupting the periodicity of the crystal lattice, and have been used extensively on a range of semiconductor applications.[35, 36] In the case of filamentary-type memristors, defect properties like concentration, defect trap-levels, or  $E_a$ , modulate the device conduction processes. An efficient control of defects enable the engineering of critical device metrics like number of conductance levels, electroforming voltage and retention and endurance.<sup>[3]</sup> Engineered defect types that control the ionic transport in filamentary-type memristors can be classified under three categories (i) intrinsic point defects: e.g.,  $V_{o}$ s and metal interstitials, (ii) extrinsic point defects: e.g., metal cations and dopants, and (iii) extended defects: e.g., dislocation networks and grain boundaries (GB).

#### Intrinsic point defects

Intrinsic point defects constitute singular lattice disruptions that are caused by the misplacement of native atoms in the host lattice. Depending on the site occupation of the defect, they can take the form of a (i)vacancy, (ii) interstitial, or (iii) substitutional (antisite).

Among these defect types,  $V_o$  is a predominant example that drive the resistive-switching process of anion-type memristors. This section provides a detailed look into  $V_o$  defects, and concludes with a discussion on other intrinsic defect types.



#### Oxygen vacancies (V)

Conduction mechanism  $V_o$ s can contribute to the electron transport dynamics of anion-type memristors through three mechanisms: (i)  $V_o$  induced defect levels within the band gap, (ii) modulation of Schottky barrier between the oxide and metal-electrode, and (iii) formation of CFs with high  $V_o$  concentrations.<sup>[37]</sup>

In  $V_o$  induced defect levels, the underlying conduction processes are governed by the position of the defect level in reference to the band edges. Shallow defect levels can contribute to the electron conduction by thermal excitation of electrons into the conduction band via Poole-Frenkel (PF) mechanism. [38] When defect levels are located deeper in the bandgap, they can act as traps for electrons and holes. In this case, thermal excitation does not provide enough energy to excite electrons into the conduction band, and electrons are transported via Trap-to-Trap tunneling (TAT) mechanism during conduction. Another frequently reported conduction mechanism is Space-Charge-Limited-Conductance (SCLC).[39] SCLC considers limitation of electron conductivity by the space charge layer formed by injected electrons in the dielectric. SCLC is governed by electron injection dynamics across the electrodes as a function of voltage bias, and density and energy-levels of traps.

PF, TAT and SCLC mechanisms can be distinguished through the relation between the current density and electric field. Further insight into trap energy-levels can be obtained from the Arrhenius plots of current density. In the literature, it has been proposed that resistive-switching can originate due to transitions between different conduction mechanisms as a function of the energy distribution of traps, trap density and number of injected charge carriers. However, it is important to note that, a significant shortcoming of the widely reported trap-assisted electron conduction mechanisms via PF, TAT or TC-SCLC, is the assumption that the defect distribution is homogeneous under constant voltage bias. This assumption does not reflect the rich defect properties of anion-type memristor devices, therefore, may render them insufficient to capture the complete bipolar resistive-switching cycle. [39, 40]

 $V_o$ s can also contribute to the conduction process by modulating the Schottky barrier at the interface of metal-oxide and ME. As the  $V_o$  concentration is often inhomogeneous across the MEs of the memristor device,  $V_o$  dynamics at the metaloxide interface can significantly modify the Schottky barrier. Charged  $V_o$ s can alter the width of the Schottky barrier, while trap-induced energy levels can modulate the electron transport through it.<sup>[5]</sup> Choi et al and Yong et al recently presented the effect of  $V_o$  modified Schottky barriers on the resistive switching dynamics of CuO and  $HfO_x$  devices.<sup>[41,42]</sup>

Lastly,  $V_o$ s are critical in the formation of CFs. Although trap-assisted, and Schottky barrier limited conduction mechanisms are important when discussing the role of  $V_o$ s for high and intermediate resistance states (prior to the complete CF formation), upon its completion, CF dominates the electrical properties of the device often via ohmic conduction. When

 $V_o$  concentration in a nanometer-scale CF exceeds  $10^{21}cm^{-3}$ , overlapping of neutral  $V_o$  induced defect-levels create an electronic conduction path that mimics the ohmic conduction in LRS. [43] First-principles calculations show that  $V_o$ s are often the most energetically favorable and mobile defect structures in metal oxides. [44] Additionally, they are shown to be stable in positively charged states. These features enable  $V_o$ s to form CFs across the memristor electrodes via formation, charge evolution and electric-field induced migration processes. A recent study by Lee et al. proposes that, consecutive drift and charge-transition processes participate in the CF formation, to overcome the repulsive forces between  $V_o^{+2}$ . [32] Molecular dynamics simulations also confirm that CFs in anion-type memristors form and dissociate, as a result of  $V_o$  movements within the switching material. [45]

**Characterization of**  $V_o$ **s**  $V_o$  characterization can take two approaches: (i) theoretical methods based on first principle calculations, and (ii) experimental methods using microscopy, spectroscopy and electrical measurements.

Theoretical methods based on first-principle calculations are instrumental in determining the energy levels introduced by  $V_o$ s. As noted earlier, these energy levels govern the dominant electron-conduction mechanism in TMO filamentary memristor devices

Recent work of Alam et al. reports that, for different allotropes of  $HfO_2$ ,  $V_o$ s can form a range of shallow and deep defect states between 0.1 eV to 2 eV below CBM, while interstitial oxygen atoms create deeper levels at 2.75–3.25 eV band. [46]. A follow-up work by Kaiser et al. investigate a broader stoichiometry range of  $HfO_{2-x}$ , and report  $HfO_{2-x}$  films ranging from insulating to metallic phase, grown under decreasing oxidation conditions. [47] The change in the electrical properties of sub-stoichiometric films are shown to be a result of increasing contribution by the continuous midgap vacancy defect states in band structure.

Experimental methods focus on observing the manifestations of defects. A predominant method used experimental  $V_o$  characterization is X-ray photoelectron spectroscopy (XPS) - a standard non-destructive technique that can characterize the chemical composition and electronic structure while providing insights of defect and disorders. Studies using XPS show that, in the presence of detectable-level  $V_o$ s, metal-4f and valence band spectra can provide useful insights on  $V_o$  concentration and associated defect energy-levels. [48,49]

Figure 3 presents representative Ta-4f and valence band XPS spectra of the stoichiometric  $Ta_2O_5$ , and sub-stoichiometric  $TaO_x$  films. As the oxygen deficiency of the plasma-enhanced ALD grown  $TaO_x$  films increases,  $Ta-4f_{7/2}$  line in Ta-4f spectrum shifts to higher binding energies, and slightly broadens as a result of the increasing  $V_o$  concentration. When  $V_o$  concentration increases over a certain threshold, a secondary peak attributed to  $Ta^{+4}$  oxidation state appears in the spectrum. [Fig. 3(b)] This is in contast to Thermal ALD grown stoichiometric  $Ta_2O_5$  in [Fig. 3(a)],

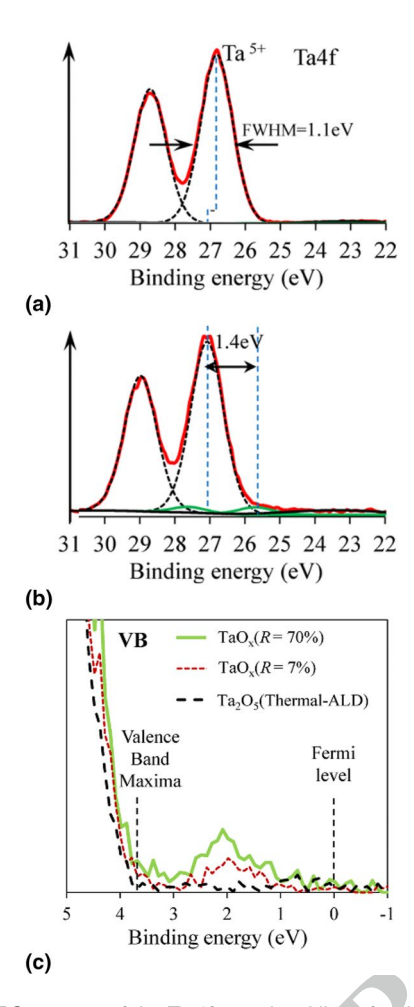


Figure 3. XPS spectra of the Ta 4f core-level lines for the stoichiometric  $Ta_2O_5$  (thermal-ALD) (a), sub-stoichiometric  $TaO_X$  (b), and XPS Valence Band Spectra of  $Ta_2O_5$ , and sub-stochiometric  $TaO_X$ films [Taken with permission from [50] Copyright 2022 American Chemical Society].

which does not exhibit these features.<sup>[50]</sup> In parallel, valence band spectra presents an additional peak above VBM, which is attributed to the defect levels of  $V_o$ s. [Fig. 3(c)] The defect levels are located between the VBM and Fermi level, 2 eV above VBM.

In addition to XPS, a range of electrical and spectroscopy measurements, e.g., Deep Level Transient Spectroscopy, Capacitance-Voltage Measurements, Low-Frequency-Noise Spectroscopy, Photoluminescence and UV-Spectroscopy, are conducted to characterize the defect induced trap levels and the density of traps in metal-oxide materials.<sup>[51–54]</sup> Although important insights like trap levels, trap activation energy, capture cross-sections can be extracted from these measurements, it is not always straightforward to correlate specific defects with measured quantities, which is where first principles computations can help.

Lastly, a variety of microscopy techniques are employed to demonstrate the formation and evolution of  $V_o$ s in anion-type

**Table I.** Neutral Defect Formation Energies of  $V_0$ .

Compound <sup>1</sup>	$\Delta H(V_0)$ O-rich (eV)	$\Delta H(V_0)$ M-rich (eV)
m-Hf0 <sub>2</sub>	6.43	0.41
$o-HfO_2$	6.42	0.41
$m-\text{TiO}_2$	4.17	-1.06
$o-TiO_2$	4.88	-0.37
$m-{\rm Ta}_2{\rm O}_5$	5.26	0.58
o-Ta <sub>2</sub> 0 <sub>5</sub>	6.01	1.36

<sup>1</sup>All structures are obtained from Materials Project.<sup>[25]</sup>

memristors, and investigate their role in memristor switching dynamics. Despite the inherent challenges associated with the  $V_o$  observation, there are several efforts that directly or indirectly probe  $V_o$  dynamics, e.g., correlation of local stoichiometry changes with  $V_o$  concentration. [55] In-situ studies are especially indispensable to reveal atomic-scale processes of resistive-switching. For example, Gao et al. and Cooper et al. demonstrate EELS coupled in-situ TEM studies that showcase electric-field induced oxygen migration process, and the role of oxygen evolution and reincorporation responsible for the resistive-switching phenomena in CeO2, and SrTiO3 systems, respectively. [56,57] Li et al utilize in-situ electron holography to correlate local  $V_o$  concentration changes with the CF formation. [20] Celano et al use scalpel scanning probe microscopy technique to investigate CF evolution throughout the memristor with a specific focus on the oxygen exchange layer.<sup>[58]</sup>

**Defect-engineering of**  $V_o$ s  $V_o$  engineering offers a versatile strategy to effectively tune the electronic properties of TMOs, which would in turn modulate the resistive-switching dynamics of TMO memristors. One of the critical parameters for vacancy engineering is  $V_o$  formation energy  $(\Delta H(V_O))$ , which represents the thermodynamic likelihood of formation of  $V_o$ s.  $\Delta H(V_O)$  has an exponential relation with the vacancydefect concentration. Under thermodynamic equilibrium, and in the dilute limit, defect concentration can be defined as  $C = N_{sites} * exp(-\Delta H(V_O)/k_{BT})$  where  $N_{sites}$  is the number of available defect sites,  $\Delta H(V_O)$  is the formation energy,  $k_B$  is the Boltzmann constant and T is the temperature. [59]

To demonstrate  $\Delta H(V_O)$  dependency on material structure, we used DFT to calculate neutral  $\Delta H(V_O)$  in a representative case study. The study uses the 2 lowest energy phases of 3 commonly reported resistive switching oxides, namely HfO<sub>2</sub>, Ta<sub>2</sub>O<sub>5</sub>, and TiO<sub>2</sub>. The results are presented in Table 1. All structures were adopted from the Materials Project. [25] Our results indicate that  $\Delta H(V_O)$  can be modified as a function of the film stoichiometry, and metal-rich conditions lead to much lower  $\Delta H(V_O)$ . This is to be expected, as Hf, Ti and Ta are metals with high oxygen affinities, and likely to scavenge oxygen from TMO lattice while creating  $V_o$ s. Among the three, Ti has the



highest oxygen affinity, [44] which explains negative  $\Delta H(V_O)$ s for M-rich TiO<sub>2</sub>, that might lead to spontaneous formation of  $V_O$ s without an external driving force. O-rich TiO<sub>2</sub>  $\Delta$ H( $V_O$ )s are in accordance with previously calculated  $\Delta H(V_O)$ s for rutile and anatase phase TiO<sub>2</sub>. [60] Our results on HfO<sub>2</sub> agree to a large extent with the recent study by Alam et al for oxygen-rich conditions, but we report lower  $\Delta H(V_O)$ s for metal-rich films. [46] Unlike HfO<sub>2</sub>, for Ta<sub>2</sub>O<sub>5</sub> and TiO<sub>2</sub>, crystal structure becomes an important parameter that impacts the  $\Delta H(V_O)$ , where monoclinic crystal structures lead to lower  $\Delta H(V_O)$ .

Our findings confirm that  $V_o$  concentration can be engineered by controlling the stoichiometry and crystal structure of the TMO films. These metrics similarly would also drive a change in  $E_a$  of  $V_o$ , which is the energy required for defects to migrate across two available lattice sites. [61]  $\Delta H(V_Q)$  and  $E_a$  are critical thermodynamic and kinetic parameters that govern the formation and rupture of the CF, which determines the resistiveswitching dynamics, as well as the retention and endurance characteristics. [62] For example, a negative formation energy can induce multiple CF formation events and cause large variability in the resulting LRS levels.<sup>[63]</sup>

Stoichiometry and crystal structure of TMO films can be modified by varying processing conditions of the thin film deposition (i.e., temperature, oxygen partial pressure, postdeposition annealing). [64-66] In addition to these process engineering efforts, recent literature investigates more focused and controllable approaches like layer engineering, doping and use of extended defects-e.g., GBs.

In the following sections, we will elaborate on these focused  $V_o$  engineering strategies to control resistive-switching dynamics.

Layer engineering Layer engineering is a promising  $V_0$  engineering technique, where film stacks with varying  $\Delta H(V_O)$  and  $E_a$  can be designed to function as  $V_o$  source & sink regions, and oxygen migration limiting barriers. [10, 13,29] This method allows each layer to be separately engineered for a specific function, and enables a better control of the filament formation process for enhanced device performance. A common goal for this kind of studies is to confine the CF in the more-resistive (oxygen-rich) layer for a more controllable filament formation process.<sup>[32]</sup> Engineered layer components are also reported to modify HRS conduction mechanism, and modify the Joule heating process during device operation. [67]

Another layer engineering strategy is to introduce an intermediate metal layer, with high oxygen affinity, between the top-ME and switching oxide layer. [68,69] This intermediate layer, referred as oxygen exchange layer or oxygen scavenger, is shown to play a critical role in  $V_o$  formation dynamics during resistive-switching while acting as a barrier between environmental oxygen and the switching oxide layer. Recent computational and in-situ studies investigate the transformation of this intermediate layer into a sub-stoichiometric oxide, and its role as an  $V_o$  reservoir as its thickness, stoichiometry and crystal structure change during the switching process.<sup>[58,70]</sup> It has been also reported that, intermediate metal's oxygen

scavenging capability, and resulting  $V_o$  concentration profile, can be used to tailor memristor reliability metrics: i.e., endurance and retention.[71]

An alternative strategy is to transfer the function of intermediate layer to the top-ME, which can be used to scavenge oxygen from the metal oxide layer, and create an  $V_0$ reservoir. Recent work by Yang et al. studies different oxygen scavenging capabilities of TiN electrodes fabricated by physical vapor (PVD) and atomic layer deposition (ALD) in ITO/HfO<sub>x</sub>/TiN memristors.<sup>[42]</sup> PVD device exhibits lower V<sub>FORM</sub>, and higher V<sub>SET</sub> & V<sub>RESET</sub>, in addition to a wider distribution of the latter. The notable difference in the resistive-switching characteristics is explained by different oxygen scavenging capabilities of PLD and ALD TiN due to structural differences, and resulting  $V_o$  concentration profile in addition to the modified Schottky barrier.

Despite expanding the device design parameters and enhancing the control in CF formation process, increasing the number of layers in device stack may complicate the fabrication process and exacerbate the processing related variability concerns. As an alternative technique, microstructure engineering is proposed to confine the CF formation in extended defects.

Extended defects Extended defects are linear and planar level distortions in the crystal lattice. Their inherent disorder renders them preferred sites for point-defect formation and transport. A common example of this defect type is GBs. GBs are known to act as sinks for point defects, and provide low-barrier diffusion paths.<sup>[72]</sup>

First principles studies supported by in-situ scanning probe microscopy report GBs to be more conductive than the grains, due to the lower oxygen-vacancy diffusion barrier energies compared to the bulk. [73,74] Consequently, GBs can act as CF paths via diffusion of charged  $V_o$ s, and through an extensive microstructure engineering, GBs can serve as controlled CF paths.

Another example of extended defect mediated resistive switching is demonstrated for SrTiO<sub>3</sub>. Szot et al. demonstrated that dislocations in crystalline SrTiO<sub>3</sub> act as predefined CFs, and drive resistive-switching through defect mediated oxygen-transport process.<sup>[75]</sup>

Doping Doping has also been explored as a possible strategy for oxygen-vacancy engineering. Introduction of elemental dopants in TMO lattice affects both  $\Delta H(V_O)$  and  $E_a$ , and is shown to modulate memristor device performance metrics.<sup>[76]</sup> Compared to the deposition condition or device stack engineering driven methods, extrinsic doping driven  $V_o$ engineering could offer a more systematic approach that can be tailored using the first-principles calculations of atomicscale processes. Jiang et al. recently reported that  $V_0$  formation energy can change depending on the valence charge state of the dopants. P-type dopants are shown to reduce  $\Delta H(V_O)$ for both neutral and charged vacancies significantly, while n-type dopants only had the opposite effect for positively charged  $V_0$ s. [63] Schmitt et al. perform a systematic dopant

concentration study where they observe the effect of Gd doping on  $V_o$  concentration and mobility. By varying the doping concentration over a wide solubility range, they study the correlation between the congurations of  $V_o$  defects (in free or clustered settings) and resistive-switching dynamics.<sup>[77]</sup> Si doping of Ta<sub>2</sub>O<sub>5</sub> is also employed to control the mobility of  $V_0$ s by modifying the hopping distance between adjacent vacancy sites.[78]

#### Other intrinsic defect examples

Despite the majority of anion-type memristor studies attributing the mobile defect functionality to oxygen anions/vacancies, recent literature emphasize the contribution of another intrinsic point defect type "metal atom interstitials" in resistive switching process. [24,79] Wedig et al. used in situ STM analysis coupled with X-ray spectroscopy to demonstrate that both  $V_o$ s, and metal cations migrating through interstitial sites are involved in the resistive switching dynamics of  $TaO_x$ ,  $HfO_x$  and  $TaO_x$  memristors.<sup>[80]</sup> However, due to the high oxidation tendency of transition metals, filament formation via metal cations become the dominant mechanism, only if  $V_o$  concentration is engineered to be low enough. This has been achieved by post-deposition annealing of TiO<sub>2</sub> films at high temperatures under oxygen atmosphere, [65] or via introduction of a carbon/graphene layer at Ta/Ta<sub>2</sub>O<sub>5</sub> interface, in order to impede the formation of oxygen deficient  $TaO_x$  layer. [81]

#### Extrinsic point defects

Extrinsic point defects are formed by the introduction of impurity atoms in the host material lattice. Extrinsic point defects can occupy (i) interstitial, or (ii) substitutional lattice sites. Electrochemically active metal cations are the dominant extrinsic point defects that govern the resistive switching dynamics of cation-type memristors.

#### Metal cation defects

Conduction mechanism Switching dynamics of cation-type memristors are governed by the redox reactions at metal-electrolyte interfaces, and ion-transport. The switching process can be analyzed in three steps<sup>[82]</sup>: (i) Anodic dissolution of active-ME: Upon application of a sufficiently high positive voltage at electrochemically active-ME (i.e., Cu or Ag), metal cations are released from the positive electrode (anode) of the memristor. (ii) Ion-transport through solid-electrolyte: Formed metal cations diffuse and drift through a defect-mediated transport in the insulator layer that serve as a solid-electrolyte. (iii) Reduction of metal cations and deposition: Metal cations are reduced to neutral metal atoms by the electrons provided by the inert, negative electrode (cathode), and form the metallic CF through nucleation and growth steps. Upon completion of CF, a conductive bridge is formed across the two electrodes, and memristor switches to the LRS. Transition back to HRS occurs via electrochemical dissolution of the filament following the application of reversed voltage (positive) at the inert-ME.

CF formation and dissolution dynamics are critical to better understand and control cation-type memristor switching dynamics. Rate-limiting processes can occur at the reductionoxidation or ion transport step.

Pioneering works by Yang et al demonstrated the complimentary roles of these two mechanisms using ex-situ and insitu TEM studies of cation-type memristors. [23,34] According to these studies, nucleation sites and growth direction of filaments are mainly directed by cation mobility, i.e., the rate of ion-transport; while cation supply and filament geometry are largely controlled by redox rates. Ion-transport becomes the rate-limiting process, when  $E_a$  of consecutive ion hopping steps is high. In that case, cations get reduced by injected electrons within the solid electrolyte before reaching the inert-ME, and CF becomes an extension of the active-ME. This phenomena is also reported for Cu/Al<sub>2</sub>O<sub>3</sub>/TiN devices, where low Cu<sup>+</sup> cation mobility in Al<sub>2</sub>O<sub>3</sub> medium becomes the rate-limiting process of Cu filament formation.<sup>[83]</sup>

Characterization of metal cations Metal cation dynamics that lead to resistive-switching processes can be analyzed via theoretical and experimental approaches similar to  $V_o$ characterization.

First principles-based DFT computations of defect-formation and migration barrier energies provide insights on the energy cost of introducing the metal cation to the solid electrolyte (as an extrinsic point defect), [84] and defect-mediated hopping of metal cations throughout the solid-electrolyte. [33,85] Recent work of Sassine et al. investigates  $\Delta H(Cu_i)$  and  $E_a$  of  $Cu_i$ , in HfO<sub>2</sub>,  $Ta_2O_5$ ,  $Al_2O_3$  and  $GdO_x$ , along with  $V_o$ s. [61] The study proposes that relevant device metrics like ON/OFF ratio, endurance and retention can be optimized using a materials selection process guided by insights on  $Cu_i$  and  $V_o$  formation & migration, obtained from first-principles calculations.

A joint analysis of first principle calculation results along with experimental findings will be instrumental for a detailed understanding of the resistive-switching mechanism. Cyclic voltammetry (CV) can be a valuable technique in that regard, which enables the measurement of oxidation and reduction reaction potentials of electrochemical cells.<sup>[86]</sup> In these measurements, oxidation and reduction processes manifest themselves as current density peaks in positive and negative sweep directions, respectively. Characterization of electrochemically driven cation-type memristors using the CV technique, under conditions to limit filament formation  $(V < V_{set})$ , [87] provide valuable insights into the dynamics of contributing redox reactions and rate-limiting processes. Resulting number of peaks, integrated area, along with the peak position and intensities can be used to identify the charge states of the cations, redox reactions, participating metal species, concentration and diffusion coefficient of the mobile ions.

Reported CV studies of Ta<sub>2</sub>O<sub>5</sub>/Pt based cation-type memristors with Ag or Cu active electrodes demonstrate that Cu and Ag cations participate in the resistive-switching process in different oxidation states. Cu atoms can be oxidized to



both Cu<sup>2+</sup> and Cu<sup>1+</sup> states, while for Ag, only oxidation to Ag<sup>1+</sup> state is energetically favorable.<sup>[88]</sup> Lubben et al's extensive CV measurements of cation-type memristors with alternating MEs show that only Ag, Cu and Fe metals present comparably favorable reduction and oxidation processes in ME/SiO<sub>2</sub>/Pt material system, which renders these metals as suitable active-ME candidates.<sup>[89]</sup>

Additional characterization techniques are employed to deepen the understanding of metal cation driven CF formation. Due to the larger atomic contrast between the insulator switching medium and mobile metal cations that form the CFs, in-situ electron microscopy studies are numerous. Guo et al's early work demonstrates the bipolar resistive-switching process for Pt/H<sub>2</sub>O/Ag cation-type memristors using the in-situ SEM technique.<sup>[90]</sup> SEM images showcase the Ag dendrites formation by Ag<sup>+</sup> during the SET process, and following dissolution during the RESET. In more recent studies, HRTEM and HAADF-STEM techniques coupled with EDS and EELS analysis are used to deduce chemical composition changes and filament formation during the operation of cation-type memristors.[11,91] Extensive in-situ TEM work reported by Yang et al. was instrumental in understanding of respective roles of cation mobility and redox reaction rates on filament formation dynamics. [23,34] Scanning probe microscopes are also immensely useful in in-situ device characterization efforts. In-situ C-AFM techniques are used to correlate the local conductivity changes with morphological features and surface topography. [83,92]

**Defect-engineering of metal cations** Engineering thermodynamic and kinetic processes that guides metal cation formation and migration is critical for controlled CF evolution. Additionally, more focused efforts target confining the CF in pre-engineered pathways, e.g. dislocations.

A common engineering technique is to modify formation and mobility of Ag ions by changing the switching medium.

To showcase the impact of the switching medium material stoichiometry and structure, we used DFT to calculate the neutral  $\Delta H(Ag_i)$ , for three oxide compounds, similar to the  $\Delta H(V_o)$  calculations presented earlier. Interstitial defect position is chosen, since in similar lattice structures, interstitial  $Ag_i$  is

Table II. Neutral Defect Formation Energies of Ag<sub>i</sub>.

Compound <sup>1</sup>	$\Delta H(Ag_i)$ O-rich (eV)	ΔH(Ag <sub>i</sub> ) M-rich (eV)
m-Hf0 <sub>2</sub>	6.94	6.45
$o-Hf0_2$	6.86	6.37
$m-\text{TiO}_2$	4.70	4.22
$o-TiO_2$	2.36	1.87
m-Ta <sub>2</sub> 0 <sub>5</sub>	2.67	2.18
$o-Ta_2O_5$	4.04	3.56

<sup>&</sup>lt;sup>1</sup>All structures are obtained from Materials Project.<sup>[25]</sup>

known to be more energetically favorable than substitutional  $M_{Ag}$  sites. [93] Our results are presented in Table II.

In general, the stoichiometry effect on defect formation energies are less pronounced for  $Ag_i$  unlike the case of  $V_o$ . Among the three oxide compounds studied,  $HfO_2$  demonstrate the highest  $\Delta H(Ag_i)$  for both crystal structures. The results are in the same range with previously reported  $\Delta H(Ag_i)$  in  $HfO_2$  bulk, <sup>[94]</sup> but significantly higher than the recent work of Banerjee et al where formation energy of  $Ag_i$  pairs in  $HfO_2$  is reported. <sup>[95]</sup> Overall,  $o - TiO_2$  and  $m - Ta_2O_5$  crystal structures offer the most energetically favorable configurations for  $Ag_i$  defects. In agreement with this observation, recent experimental studies demonstrated formation and migration of  $Ag^+$  in  $Ag/Ta_2O_5/Pt$  memristors. <sup>[88]</sup>

Alloying As Ag and Cu can effectively diffuse via interstitial sites in a-Si, [96] a-Si is typically used as a switching medium/solid-electrolyte for cation-type memristors. [97,98] However, large diffusivity of these electrochemically active metals can cause significant resistive switching variation, due to multiple filament formations, and poor data retention. Recently, Yeon et al. investigated different Ag-alloys for better controlled CF formation. By engineering a selection of metals and varying compositions, authors found out that Ag-Cu alloys provide improved linear and symmetric conductance levels, in addition to superior retention properties. [99]

Extended defects Extended defects of preferential impurity diffusion paths, can be engineered to create controlled conduction pathways, where CFs will be confined. Combining an epitaxial growth technique, where defect-engineering can be performed in a systematic manner, and cation migration process can enable a superior cation-type memristor with desired device metrics. Choi et al. demonstrated that epitaxially grown SiGe films can be engineered with atomic-scale threading dislocations that can serve as controlled Ag<sup>+</sup> transport pathways. Controlling the density and width of threading dislocations, enables memristors with high endurance, long retention, and linear conductance levels. [100]

#### Other extrinsic defect examples

CF forming metal cations are not the only extrinsic defect examples that can modify memristor device characteristics. Various impurity atoms can be introduced in memristor switching medium as in the example of dopant atoms that modify vacancy formation and migration dynamics in anion-type memristors. [63] Furthermore, impurity atoms can be engineered to modulate structural, compositional and electronic properties of the switching medium: e.g., formation of additional defect levels, inducing a space-charge layer, driving crystal phase transition, or acting as donor or acceptors (i.e., dopants).

Nb is shown to act as a donor for  $SrTiO_3$  and  $BaTiO_3$ , by substituting the Ti sites (Nb<sup>+5</sup> and Ti<sup>+4</sup>) and increasing the n-type conductivity. [101-103] Doping of  $SiO_2$  with Al and Ga,

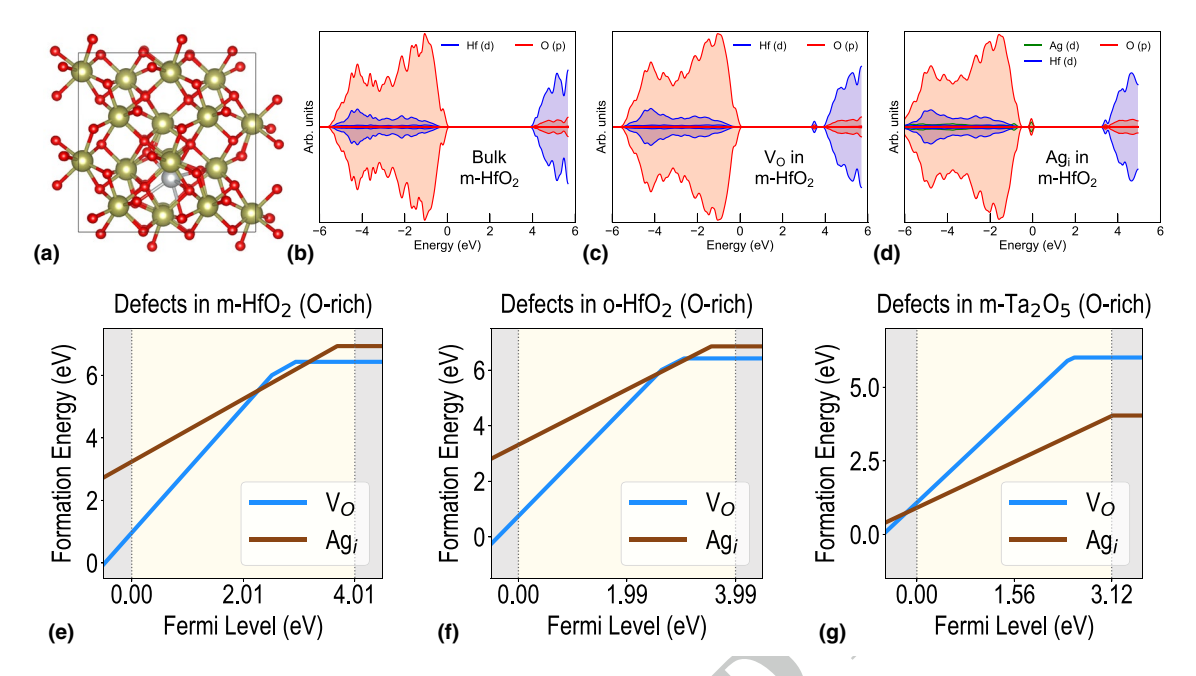


Figure 4. (a) Ag<sub>i</sub> in m-HfO<sub>2</sub> lattice, DOS of (b) Bulk m-HfO<sub>2</sub>, (c) V<sub>0</sub> in m-HfO<sub>2</sub>, and (d) Ag<sub>i</sub> in m-HfO<sub>2</sub>, Fermi level (eV)-dependent formation energies (eV) of  $V_0$  and  $Ag_i$  in (e) O-rich m-HfO<sub>2</sub>, (f) O-rich o-HfO<sub>2</sub>, (g) O-rich m-Ta<sub>2</sub>O<sub>5</sub>

modulates the solubility of Cu cations in SiO<sub>2</sub> matrix, and impacts the resistive-switching dynamics of Cu/SiO<sub>2</sub>/Pt memristors. Presence of dopants is further shown to enhance the stability of conductance levels at the cost of slowing down the switching process. [22] In-situ TEM and Atom Probe Tomography studies of Ag/TiO<sub>2</sub>/Pt memristors, demonstrated doping as a critical driver of the resistive-switching process. Ag-dopant atoms are proposed to substitute Ti atoms of anatase TiO<sub>2</sub> during the formation of anatase TiO<sub>2</sub> CF, and resistive-switching process is shown to be coupled with doping and de-doping of CF with Ag<sup>+</sup>.[104]

#### Comparison of charged intrinsic and extrinsic point defects

We performed first principles-based DFT computations to compare the likelihood of formation of charged  $V_o$ s and metal interstitials in oxides, as well as energy levels such defects may create within the band gap. [105,106]

Figure 4(a) shows the DFT optimized structure of m-HfO<sub>2</sub> with a  $Ag_i$  defect, while Fig. 4(b)–(d) show how the electronic density of states (DOS) change from bulk m-HfO<sub>2</sub> to when  $V_O$  and  $Ag_i$  are present, which lead to energy states in the band gap region. Figure 4(e-g) further show the charge and Fermi level-dependent formation energies of  $V_O$  and  $Ag_i$ in m-HfO<sub>2</sub>, o-HfO<sub>2</sub>, and m-Ta<sub>2</sub>O<sub>5</sub>, respectively. It can be deduced that both  $V_Q$  and Ag, create positively charged donortype defects in the band gap, and generally have comparable energies.  $V_O$  exhibits deep +2/+1 and +1/0 transition levels for m-HfO<sub>2</sub> and o-HfO<sub>2</sub>, and a +2/0 level for m-Ta<sub>2</sub>O<sub>5</sub>. On the other hand,  $Ag_i$  only creates shallow +1/0 levels close to the CBM and is not expected to have deep energy states like  $V_O$ . Further,  $V_O$  is lower in energy for most of the band gap region for both HfO2 structures, while Ag, has a lower energy in  $m-\text{Ta}_2\text{O}_5$ . All formation energies are positive within the band gap implying these defects may not spontaneously form under O-rich conditions, but certainly by tuning the chemical potential and creating complex defects-such as Ag, and  $V_O$  in the same structure– stability and energy levels can be suitably modified.

#### **Conclusion**

We provided a general overview of defect-engineering in resistive-switching dynamics of filamentary-type memristors. Defects are key entities that govern the formation and evolution of CFs. As such, defect-engineering can be a promising step towards memristors with controlled conduction pathways to remedy variability and endurance challenges. In order to take advantage of this technique, it is imperative to create a data driven defect-engineering framework that integrates the defect knowledge obtained via first-principles calculations within the process design parameters of the thin film deposition, through a feedback loop driven by extensive characterization results.

#### **Acknowledgments**

A.M.K. acknowledges support from the School of Materials Engineering at Purdue University under Account Number F.10023800.05.002. GT acknowledges support from Wayne State University and NSF Grant CCF-2153177.



#### **Data availability**

The datasets generated during and/or analysed during the current study are available from the corresponding author on reasonable request.

#### **Declarations**

#### **Conflict of interest**

On behalf of all authors, the corresponding author states that there is no conflict of interest.

#### References

- G.E. Moore, Cramming more components onto integrated circuits, Reprinted from Electronics, 38,(8), April 19, 1965, pp114 ff. IEEE Solid-State Circuits Soc. Newsl. 11(3), 33–35 (2006). https://doi.org/10. 1109/n-ssc.2006.4785860
- D. Ielmini, H.-S.P. Wong, In-memory computing with resistive switching devices. Nat. Electron. 1(6), 333–343 (2018). https://doi.org/10.1038/ s41928-018-0092-2
- J. Zhu, T. Zhang, Y. Yang, R. Huang, A comprehensive review on emerging artificial neuromorphic devices. Appl. Phys. Rev. 7(1), 011312 (2020). https://doi.org/10.1063/1.5118217
- Q. Xia, J.J. Yang, Memristive crossbar arrays for brain-inspired computing. Nat. Mater. 18(4), 309–323 (2019). https://doi.org/10.1038/s41563-019-0291-x
- D.B. Strukov, G.S. Snider, D.R. Stewart, R.S. Williams, The missing memristor found. Nature 453(7191), 80–83 (2008). https://doi.org/10.1038/ nature06932
- L. Chua, Memristor: the missing circuit element. IEEE Trans. Circuit Theory 18(5), 507–519 (1971). https://doi.org/10.1109/tct.1971.1083337
- L. Chua, Resistance switching memories are memristors. Appl. Phys. A 102(4), 765–783 (2011). https://doi.org/10.1007/s00339-011-6264-9
- J.J. Yang, D.B. Strukov, D.R. Stewart, Memristive devices for computing. Nat. Nanotechnol. 8(1), 13–24 (2013). https://doi.org/10.1038/nnano. 2012 240
- Y. Yang, R. Huang, Probing memristive switching in nanoionic devices. Nat. Electron. 1(5), 274–287 (2018). https://doi.org/10.1038/s41928-018-0069-1
- G.-S. Park, Y.B. Kim, S.Y. Park, X.S. Li, S. Heo, M.-J. Lee, M. Chang, J.H. Kwon, M. Kim, U.-I. Chung, R. Dittmann, R. Waser, K. Kim, In situ observation of filamentary conducting channels in an asymmetric Ta-05-x/ Ta02-x bilayer structure. Nat. Commun. 4(1), 2382 (2013). https://doi.org/10.1038/ncomms3382
- W. Sun, B. Gao, M. Chi, Q. Xia, J.J. Yang, H. Qian, H. Wu, Understanding memristive switching via in situ characterization and device modeling. Nat. Commun. 10(1), 3453 (2019). https://doi.org/10.1038/ s41467-019-11411-6
- D.-H. Kwon, K.M. Kim, J.H. Jang, J.M. Jeon, M.H. Lee, G.H. Kim, X.-S. Li, G.-S. Park, B. Lee, S. Han, M. Kim, C.S. Hwang, Atomic structure of conducting nanofilaments in TiO2 resistive switching memory. Nat. Nanotechnol. 5(2), 148–153 (2010). https://doi.org/10.1038/nnano.2009.456
- M.-J. Lee, C.B. Lee, D. Lee, S.R. Lee, M. Chang, J.H. Hur, Y.-B. Kim, C.-J. Kim, D.H. Seo, S. Seo, U.-I. Chung, I.-K. Yoo, K. Kim, A fast, high-endurance and scalable non-volatile memory device made from asymmetric Ta205-x/Ta02-x bilayer structures. Nat. Mater. 10(8), 625–630 (2011). https://doi.org/10.1038/nmat3070
- C. Chang, J. Chen, C. Huang, C. Chiu, T. Lin, P. Yeh, W. Wu, Direct observation of dual-filament switching behaviors in Ta205-based memristors. Small 13(15), 1603116 (2017). https://doi.org/10.1002/smll.201603116
- S. Pi, C. Li, H. Jiang, W. Xia, H. Xin, J.J. Yang, Q. Xia, Memristor crossbar arrays with 6-nm half-pitch and 2-nm critical dimension. Nat. Nanotechnol. 14(1), 35–39 (2019). https://doi.org/10.1038/s41565-018-0302-0

- M. Zhao, B. Gao, J. Tang, H. Qian, H. Wu, Reliability of analog resistive switching memory for neuromorphic computing. Appl. Phys. Rev. 7(1), 011301 (2020). https://doi.org/10.1063/1.5124915
- W. Song, H.K. Lee, W. Wang, M. Li, Z. Chen, J.-C. Liu, I.-T. Wang, V.Y.-Q. Zhuo, Y. Zhu, Investigation of Retention Failure Behavior in Analog RRAM Devices, in 2020 IEEE International Symposium on the Physical and Failure Analysis of Integrated Circuits, pp. 1–4 (2020)
- W. Banerjee, Q. Liu, H. Hwang, Engineering of defects in resistive random access memory devices. J. Appl. Phys. 127(5), 051101 (2020). https:// doi.org/10.1063/1.5136264
- A. Fantini, L. Goux, R. Degraeve, D.J. Wouters, N. Raghavan, G. Kar, A. Belmonte, Y.-Y. Chen, B. Govoreanu, M. Jurczak, Intrinsic Switching Variability in Hf02 RRAM. in 2013 5th IEEE International Memory Workshop, pp. 30–33 (2013). https://doi.org/10.1109/imw.2013.6582090
- C. Li, B. Gao, Y. Yao, X. Guan, X. Shen, Y. Wang, P. Huang, L. Liu, X. Liu, J. Li, C. Gu, J. Kang, R. Yu, Direct observations of nanofilament evolution in switching processes in Hf02-based resistive random access memory by in situ TEM studies. Adv. Mater. 29(10), 1602976 (2017). https://doi.org/10.1002/adma.201602976
- S.M. Hus, R. Ge, P.-A. Chen, L. Liang, G.E. Donnelly, W. Ko, F. Huang, M.-H. Chiang, A.-P. Li, D. Akinwande, Observation of single-defect memristor in an MoS2 atomic sheet. Nat. Nanotechnol. 16(1), 58–62 (2021). https://doi.org/10.1038/s41565-020-00789-w
- M. Lübben, F. Cüppers, J. Mohr, M.V. Witzleben, U. Breuer, R. Waser, C. Neumann, I. Valov, Design of defect-chemical properties and device performance in memristive systems. Sci. Adv. 6(19), 9079 (2020). https://doi.org/10.1126/sciadv.aaz9079
- Y. Yang, P. Gao, S. Gaba, T. Chang, X. Pan, W. Lu, Observation of conducting filament growth in nanoscale resistive memories. Nat. Commun. 3(1), 732 (2012). https://doi.org/10.1038/ncomms1737
- H. Jiang, L. Han, P. Lin, Z. Wang, M.H. Jang, Q. Wu, M. Barnell, J.J. Yang, H.L. Xin, Q. Xia, Sub-10 nm Ta channel responsible for superior performance of a Hf02 memristor. Sci. Rep. 6(1), 28525 (2016). https://doi.org/10.1038/srep28525
- A. Jain, S.P. Ong, G. Hautier, W. Chen, W.D. Richards, S. Dacek, S. Cholia, D. Gunter, D. Skinner, G. Ceder, K.A. Persson, Commentary: the materials project: a materials genome approach to accelerating materials innovation. APL Mater. 1(1), 011002 (2013). https://doi.org/10.1063/1.48123
- J.P. Perdew, K. Burke, M. Ernzerhof, Generalized gradient approximation made simple. Phys. Rev. Lett. 77(18), 3865–3868 (1996). https://doi.org/ 10.1103/physrevlett.77.3865
- P.E. Blöchl, Projector augmented-wave method. Phys. Rev. B 50(24), 17953–17979 (1994). https://doi.org/10.1103/physrevb.50.17953
- A. Marchewka, B. Roesgen, K. Skaja, H. Du, C. Jia, J. Mayer, V. Rana, R. Waser, S. Menzel, Nanoionic resistive switching memories: on the physical nature of the dynamic reset process. Adv. Electron. Mater. 2(1), 1500233 (2016). https://doi.org/10.1002/aelm.201500233
- Z. Wang, M. Yin, T. Zhang, Y. Cai, Y. Wang, Y. Yang, R. Huang, Engineering incremental resistive switching in TaO x based memristors for braininspired computing. Nanoscale 8(29), 14015–14022 (2016). https://doi. org/10.1039/c6nr00476h
- S. Yu, X. Guan, H.-S.P. Wong, On the stochastic nature of resistive switching in metal oxide RRAM: physical modeling, monte carlo simulation, and experimental characterization. in International Electron Devices Meeting 2011, 17–311734 (2011). https://doi.org/10.1109/iedm.2011.6131572
- S. Kim, S. Choi, W. Lu, Comprehensive physical model of dynamic resistive switching in an oxide memristor. ACS Nano 8(3), 2369–2376 (2014). https://doi.org/10.1021/nn405827t
- J. Lee, W. Schell, X. Zhu, E. Kioupakis, W.D. Lu, Charge transition of oxygen vacancies during resistive switching in oxide-based RRAM. ACS Appl. Mater. Interfaces 11(12), 11579–11586 (2019). https://doi.org/10.1021/acsami.8b18386
- S. Clima, K. Sankaran, Y.Y. Chen, A. Fantini, U. Celano, A. Belmonte, L. Zhang, L. Goux, B. Govoreanu, R. Degraeve, D..J. Wouters, M. Jurczak, W. Vandervorst, S..D. Gendt, G. Pourtois, RRAMs based on anionic and cationic switching: a short overview: RRAMs based on anionic and cationic switching: a short overview. Physica Status Solidi 8(6), 501–511 (2014). https://doi.org/10.1002/pssr.201409054

- 34. Y. Yang, P. Gao, L. Li, X. Pan, S. Tappertzhofen, S. Choi, R. Waser, I. Valov, W.D. Lu, Electrochemical dynamics of nanoscale metallic inclusions in dielectrics. Nat. Commun. 5(1), 4232 (2014). https://doi.org/10.1038/ ncomms5232
- 35. S.T. Pantelides, The electronic structure of impurities and other point defects in semiconductors. Rev. Mod. Phys. 50(4), 797-858 (1978). https:// doi.org/10.1103/revmodphys.50.797
- 36. H.J. Queisser, E.E. Haller, Defects in semiconductors: some fatal. Some Vital. Sci. 281(5379), 945-950 (1998). https://doi.org/10.1126/science.
- 37. W. Li, J. Shi, K.H.L. Zhang, J.L. MacManus-Driscoll, Defects in complex oxide thin films for electronics and energy applications; challenges and opportunities. Mater. Horiz. 7(11), 2832-2859 (2020). https://doi.org/10. 1039/d0mh00899k
- 38. F.-C. Chiu, A review on conduction mechanisms in dielectric films. Adv. Mater. Sci. Eng. **2014**, 1–18 (2014). https://doi.org/10.1155/2014/578168
- 39. C. Funck, S. Menzel, Comprehensive model of electron conduction in oxidebased memristive devices. ACS Appl. Electron. Mater. 3(9), 3674-3692 (2021). https://doi.org/10.1021/acsaelm.1c00398
- 40. H. Schroeder, Poole-Frenkel-effect as dominating current mechanism in thin oxide films-An illusion?! J. Appl. Phys. 117(21), 215103 (2015). https:// doi.org/10.1063/1.4921949
- 41. S.-J. Choi, G.-S. Park, K.-H. Kim, W.-Y. Yang, H.-J. Bae, K.-J. Lee, H.-I. Lee, S.Y. Park, S. Heo, H.-J. Shin, S. Lee, S. Cho, In situ observation of vacancy dynamics during resistance changes of oxide devices. J. Appl. Phys. 110(5), 056106 (2011). https://doi.org/10.1063/1.3626816
- 42. Z. Yong, K.-M. Persson, M.S. Ram, G. D'Acunto, Y. Liu, S. Benter, J. Pan, Z. Li, M. Borg, A. Mikkelsen, L.-E. Wernersson, R. Timm, Tuning oxygen vacancies and resistive switching properties in ultra-thin HfO2 RRAM via TiN bottom electrode and interface engineering. Appl. Surf. Sci. 551, 149386 (2021). https://doi.org/10.1016/j.apsusc.2021.149386
- 43. M. Saadi, P. Gonon, C. Vallée, C. Mannequin, H. Grampeix, E. Jalaguier, F. Jomni, A. Bsiesy, On the mechanisms of cation injection in conducting bridge memories: the case of HfO2 in contact with noble metal anodes (Au, Cu, Ag). J. Appl. Phys. **119**(11), 114501 (2016). https://doi.org/10.1063/1.4943776
- 44. S. Clima, Y.Y. Chen, C.Y. Chen, L. Goux, B. Govoreanu, R. Degraeve, A. Fantini, M. Jurczak, G. Pourtois, First-principles thermodynamics and defect kinetics guidelines for engineering a tailored RRAM device. J. Appl. Phys. 119(22), 225107 (2016). https://doi.org/10.1063/1.4953673
- 45. M.L. Urquiza, M.M. Islam, A.C.T.V. Duin, X. Cartoixa, A. Strachan, Atomistic insights on the full operation cycle of a Hf02-based resistive random access memory cell from molecular dynamics. ACS Nano 15(8), 12945-12954 (2021). https://doi.org/10.1021/acsnano.1c01466
- 46. M.N.K. Alam, S. Clima, B.J. O'Sullivan, B. Kaczer, G. Pourtois, M. Heyns, J.V. Houdt, First principles investigation of charge transition levels in monoclinic, orthorhombic, tetragonal, and cubic crystallographic phases of HfO2. J. Appl. Phys. 129(8), 084102 (2021). https://doi.org/10.1063/5.0033957
- 47. N. Kaiser, T. Vogel, A. Zintler, S. Petzold, A. Arzumanov, E. Piros, R. Eilhardt, L. Molina-Luna, L. Alff, Defect-stabilized substoichiometric polymorphs of hafnium oxide with semiconducting properties. ACS Appl. Mater. Interfaces 14(1), 1290-1303 (2022). https://doi.org/10.1021/acsami.1c09451
- 48. Y.Y. Lebedinskii, A.G. Chernikova, A.M. Markeev, D.S. Kuzmichev, Effect of dielectric stoichiometry and interface chemical state on band alignment between tantalum oxide and platinum. Appl. Phys. Lett. 107(14), 142904 (2015). https://doi.org/10.1063/1.4932554
- 49. T.V. Perevalov, V.S. Aliev, V.A. Gritsenko, A.A. Saraev, V.V. Kaichev, Electronic structure of oxygen vacancies in hafnium oxide. Microelectron. Eng. 109, 21-23 (2013). https://doi.org/10.1016/j.mee.2013.03.005
- 50. K.V. Egorov, D.S. Kuzmichev, P.S. Chizhov, Y.Y. Lebedinskii, C.S. Hwang, A..M.. Markeev, In situ control of oxygen vacancies in TaO x thin films via plasma-enhanced atomic layer deposition for resistive switching memory applications. ACS Appl. Mater. Interfaces 9(15), 13286-13292 (2017). https://doi.org/10.1021/acsami.7b00778
- 51. A. Kumar, S. Mondal, K.S.R.K. Rao, Experimental evidences of charge transition levels in ZrO2 and at the Si: ZrO2 interface by deep level transient spectroscopy. Appl. Phys. Lett. 110(13), 132904 (2017). https://doi.org/10. 1063/1.4979522
- 52. K. Sugawara, H. Shima, M. Takahashi, Y. Naitoh, H. Suga, H. Akinaga, Lowfrequency-noise spectroscopy of TaOx-based resistive switching memory.

- Adv. Electron. Mater. 2021, 2100758 (2021). https://doi.org/10.1002/aelm.
- 53. X. Wang, B. Gao, H. Wu, X. Li, D. Hong, Y. Chen, H. Qian, A nondestructive approach to study resistive switching mechanism in metal oxide based on defect photoluminescence mapping. Nanoscale 9(36), 13449-13456 (2017). https://doi.org/10.1039/c7nr02023f
- V.A. Gritsenko, T.V. Perevalov, D.R. Islamov, Electronic properties of hafnium oxide: a contribution from defects and traps. Phys. Rep. 613, 1–20 (2016). https://doi.org/10.1016/j.physrep.2015.11.002
- 55. J. Chen, C. Huang, C. Chiu, Y. Huang, W. Wu, Switching kinetic of VCMbased memristor: evolution and positioning of nanofilament. Adv. Mater. 27(34), 5028-5033 (2015). https://doi.org/10.1002/adma.201502758
- 56. P. Gao, Z. Wang, W. Fu, Z. Liao, K. Liu, W. Wang, X. Bai, E. Wang, In situ TEM studies of oxygen vacancy migration for electrically induced resistance change effect in cerium oxides. Micron 41(4), 301-305 (2010). https://doi.org/10.1016/j.micron.2009.11.010
- 57. D. Cooper, C. Baeumer, N. Bernier, A. Marchewka, C.L. Torre, R.E. Dunin-Borkowski, S. Menzel, R. Waser, R. Dittmann, Anomalous resistance hysteresis in oxide ReRAM: oxygen evolution and reincorporation revealed by in situ TEM. Adv. Mater. 29(23), 1700212 (2017). https://doi.org/10. 1002/adma.201700212
- 58. U. Celano, J..O..d Beeck, S. Clima, M.. Luebben, P..M.. Koenraad, L.. Goux, I. Valov, W.. Vandervorst, Direct probing of the dielectric scavenging-layer interface in oxide filamentary-based valence change memory. ACS Appl. Mater. Interfaces 9(12), 10820-10824 (2017). https://doi.org/ 10.1021/acsami.6b16268
- C..G., V..d Walle, A. Janotti, Advances in electronic structure methods for defects and impurities in solids. Physica Status Solidi (b) 248(1), 19-27 (2011). https://doi.org/10.1002/pssb.201046290
- H. Cheng, A. Selloni, Surface and subsurface oxygen vacancies in anatase TiO2 and differences with rutile. Phys. Rev. B 79(9), 092101 (2009). https://doi.org/10.1103/physrevb.79.092101
- 61. G. Sassine, C. Nail, P. Blaise, B. Sklenard, M. Bernard, R. Gassilloud, A. Marty, M. Veillerot, C. Vallée, E. Nowak, G. Molas, Hybrid-RRAM toward next generation of nonvolatile memory: coupling of oxygen vacancies and metal ions. Adv. Electron. Mater. 5(2), 1800658 (2019). https://doi. org/10.1002/aelm.201800658
- 62. H. Jiang, D.A. Stewart, Enhanced oxygen vacancy diffusion in Ta205 resistive memory devices due to infinitely adaptive crystal structure. J. Appl. Phys. 119(13), 134502 (2016). https://doi.org/10.1063/1.4945579
- 63. H. Jiang, D.A. Stewart, Using dopants to tune oxygen vacancy formation in transition metal oxide resistive memory. ACS Appl. Mater. Interfaces 9(19), 16296-16304 (2017). https://doi.org/10.1021/acsami.7b00139
- 64. W. He, H. Sun, Y. Zhou, K. Lu, K. Xue, X. Miao, Customized binary and multilevel HfO2-x-based memristors tuned by oxidation conditions. Sci. Rep. 7(1), 10070 (2017). https://doi.org/10.1038/s41598-017-09413-9
- 65. J. Ge, M. Chaker, Oxygen vacancies control transition of resistive switching mode in single-crystal TiO2 memory device. ACS Appl. Mater. Interfaces 9(19), 16327-16334 (2017). https://doi.org/10.1021/acsami.7b03527
- S.U. Sharath, T. Bertaud, J. Kurian, E. Hildebrandt, C. Walczyk, P. Calka, P. Zaumseil, M. Sowinska, D. Walczyk, A. Gloskovskii, T. Schroeder, L. Alff, Towards forming-free resistive switching in oxygen engineered HfO2-x. Appl. Phys. Lett. 104(6), 063502 (2014). https://doi.org/10.1063/1.4864653
- 67. A. Hardtdegen, C.L. Torre, F. Cüppers, S. Menzel, R. Waser, S. Hoffmann-Eifert, Improved switching stability and the effect of an internal series resistor in Hf02/TiOx bilayer ReRAM cells. IEEE Trans. Electron Devices 65(8), 3229-3236 (2018). https://doi.org/10.1109/ted.2018.2849872
- 68. X. Zhong, I. Rungger, P. Zapol, H. Nakamura, Y. Asai, O. Heinonen, The effect of a Ta oxygen scavenger layer on HfO 2 -based resistive switching behavior: thermodynamic stability, electronic structure, and low-bias transport. Phys. Chem. Chem. Phys. 18(10), 7502-7510 (2016). https://doi.org/10. 1039/c6cp00450d
- 69. W. Kim, S. Menzel, D.J. Wouters, Y. Guo, J. Robertson, B. Roesgen, R. Waser, V. Rana, Impact of oxygen exchange reaction at the ohmic interface in Ta205 -based ReRAM devices. Nanoscale 8(41), 17774-17781 (2016). https://doi.org/10.1039/c6nr03810g
- 70. D.-Y. Cho, M. Luebben, S. Wiefels, K.-S. Lee, I. Valov, Interfacial metal-oxide interactions in resistive switching memories. ACS Appl. Mater. Interfaces 9(22), 19287-19295 (2017). https://doi.org/10.1021/acsami.7b02921



- 71. Y.Y. Chen, L. Goux, S. Clima, B. Govoreanu, R. Degraeve, G.S. Kar, A. Fantini, G. Groeseneken, D.J. Wouters, M. Jurczak, Endurance/retention trade-off on HfO2/metal cap 1T1R bipolar RRAM. IEEE Trans. Electron Devices 60(3), 1114-1121 (2013). https://doi.org/10.1109/ted.2013.2241064
- 72. O. Pirrotta, L. Larcher, M. Lanza, A. Padovani, M. Porti, M. Nafría, G. Bersuker, Leakage current through the poly-crystalline Hf02: trap densities at grains and grain boundaries. J. Appl. Phys. 114(13), 134503 (2013). https://doi.org/10.1063/1.4823854
- 73. V. Iglesias, M. Lanza, K. Zhang, A. Bayerl, M. Porti, M. Nafría, X. Aymerich, G. Benstetter, Z.Y. Shen, G. Bersuker, Degradation of polycrystalline HfO2based gate dielectrics under nanoscale electrical stress. Appl. Phys. Lett. 99(10), 103510 (2011), https://doi.org/10.1063/1.3637633
- 74. G. Bersuker, J. Yum, L. Vandelli, A. Padovani, L. Larcher, V. Iglesias, M. Porti, M. Nafría, K. McKenna, A. Shluger, P. Kirsch, R. Jammy, Grain boundarydriven leakage path formation in Hf02 dielectrics. Solid-State Electron. 65, 146-150 (2011). https://doi.org/10.1016/j.sse.2011.06.031
- 75. K. Szot, W. Speier, G. Bihlmayer, R. Waser, Switching the electrical resistance of individual dislocations in single-crystalline SrTiO3. Nat. Mater. 5(4), 312-320 (2006). https://doi.org/10.1038/nmat1614
- 76. L. Zhao, S.-W. Ryu, A. Hazeghi, D. Duncan, B. Magyari-Köpe, Y. Nishi, Dopant selection rules for extrinsic tunability of hfo<inf>x</inf> rram characteristics: a systematic study. in, 2013 Symposium on VLSI Technology, pp. 106-107 (2013)
- 77. R. Schmitt, J. Spring, R. Korobko, J.L.M. Rupp, Design of Oxygen Vacancy Configuration for Memristive Systems. ACS Nano 11(9), 8881-8891 (2017). https://doi.org/10.1021/acsnano.7b03116
- 78. S. Kim, S. Choi, J. Lee, W.D. Lu, Tuning resistive switching characteristics of tantalum oxide memristors through Si doping. ACS Nano 8(10), 10262-10269 (2014). https://doi.org/10.1021/nn503464q
- 79. D. Carta, I. Salaoru, A. Khiat, A. Regoutz, C. Mitterbauer, N.M. Harrison, T. Prodromakis, Investigation of the switching mechanism in TiO2-based RRAM: a two-dimensional EDX approach. ACS Appl. Mater. Interfaces 8(30), 19605-19611 (2016). https://doi.org/10.1021/acsami.6b04919
- 80. A. Wedig, M. Luebben, D.-Y. Cho, M. Moors, K. Skaja, V. Rana, T. Hasegawa, K.K. Adepalli, B. Yildiz, R. Waser, I. Valov, Nanoscale cation motion in TaOx, HfOx and TiOx memristive systems. Nat. Nanotechnol. 11(1), 67–74 (2016). https://doi.org/10.1038/nnano.2015.221
- 81. M. Lübben, P. Karakolis, V. Ioannou-Sougleridis, P. Normand, P. Dimitrakis, I. Valov, Graphene-modified interface controls transition from VCM to ECM switching modes in Ta/TaOx based memristive devices. Adv. Mater. 27(40), 6202-6207 (2015). https://doi.org/10.1002/adma.201502574
- 82. R. Waser, R. Dittmann, G. Staikov, K. Szot, Redox-based resistive switching memories - nanoionic mechanisms, prospects, and challenges. Adv. Mater. 21(25–26), 2632–2663 (2009). https://doi.org/10.1002/adma.200900375
- U. Celano, L. Goux, A. Belmonte, K. Opsomer, A. Franquet, A. Schulze, C. Detavernier, O. Richard, H. Bender, M. Jurczak, W. Vandervorst, Three-dimensional observation of the conductive filament in nanoscaled resistive memory devices. Nano Lett. 14(5), 2401-2406 (2014). https://doi.org/10.1021/nl500049g
- 84. T. Gu, T. Tada, S. Watanabe, Conductive path formation in the Ta205 atomic switch: first-principles analyses. ACS Nano 4(11), 6477-6482 (2010). https://doi.org/10.1021/nn101410s
- 85. K. Sankaran, L. Goux, S. Clima, M. Mees, J.A. Kittl, M. Jurczak, L. Altimime, G.-M. Rignanese, G. Pourtois, Modeling of copper diffusion in amorphous aluminum oxide in CBRAM memory stack. ECS Trans. 45(3), 317-330 (2012). https://doi.org/10.1149/1.3700896
- 86. N. Elgrishi, K.J. Rountree, B.D. McCarthy, E.S. Rountree, T.T. Eisenhart, J.L. Dempsey, A practical beginner's guide to cyclic voltammetry. J. Chem. Educ. 95(2), 197-206 (2018). https://doi.org/10.1021/acs.jchemed.7b00361
- 87. S. Chen, I. Valov, Design of materials configuration for optimizing redoxbased resistive switching memories. Adv. Mater. 34(3), 2105022 (2022). https://doi.org/10.1002/adma.202105022
- 88. T. Tsuruoka, I. Valov, S. Tappertzhofen, J.V.D. Hurk, T. Hasegawa, R. Waser, M. Aono, Redox reactions at Cu, Ag/Ta205 interfaces and the effects of Ta205 film density on the forming process in atomic switch structures. Adv. Funct. Mater. 25(40), 6374-6381 (2015). https://doi.org/10.1002/ adfm.201500853
- 89. M. Lübben, I. Valov, Active electrode redox reactions and device behavior in ECM type resistive switching memories. Adv. Electron. Mater. 5(9), 1800933 (2019). https://doi.org/10.1002/aelm.201800933

- 90. X. Guo, C. Schindler, S. Menzel, R. Waser, Understanding the switching-off mechanism in Ag+ migration based resistively switching model systems. Appl. Phys. Lett. 91(13), 133513 (2007). https://doi.org/10.1063/1.27936
- 91. F. Yuan, Z. Zhang, C. Liu, F. Zhou, H.M. Yau, W. Lu, X. Qiu, H.-S.P. Wong, J. Dai, Y. Chai, Real-time observation of the electrode-size-dependent evolution dynamics of the conducting filaments in a SiO2 layer. ACS Nano 11(4), 4097-4104 (2017). https://doi.org/10.1021/acsnano.7b00783
- 92. M. Lanza, U. Celano, F. Miao, Nanoscale characterization of resistive switching using advanced conductive atomic force microscopy based setups. J. Electroceram. 39(1-4), 94-108 (2017). https://doi.org/10.1007/ s10832-017-0082-1
- 93. S. Prada, M. Rosa, L. Giordano, C.D. Valentin, G. Pacchioni, Density functional theory study of TiO2/Ag interfaces and their role in memristor devices. Phys. Rev. B 83(24), 245314 (2011). https://doi.org/10.1103/ physrevb.83.245314
- 94. M. Zhou, Q. Zhao, W. Zhang, Q. Liu, Y. Dai, The conductive path in Hf02: first principles study. J. Semicond. 33(7), 072002 (2012). https://doi.org/ 10.1088/1674-4926/33/7/072002
- W. Banerjee, S.H. Kim, S. Lee, D. Lee, H. Hwang, An efficient approach based on tuned nanoionics to maximize memory characteristics in Agbased devices. Adv. Electron. Mater. 7(4), 2100022 (2021). https://doi.org/ 10.1002/aelm.202100022
- 96. S. Coffa, J.M. Poate, D.C. Jacobson, W. Frank, W. Gustin, Determination of diffusion mechanisms in amorphous silicon. Phys. Rev. B 45(15), 8355-8358 (1991). https://doi.org/10.1103/physrevb.45.8355
- K.-H. Kim, S. Gaba, D. Wheeler, J.M. Cruz-Albrecht, T. Hussain, N. Srinivasa, W. Lu, A functional hybrid memristor crossbar-array/CMOS system for data storage and neuromorphic applications. Nano Lett. 12(1), 389-395 (2012). https://doi.org/10.1021/nl203687n
- S.H. Jo, T. Chang, I. Ebong, B.B. Bhadviya, P. Mazumder, W. Lu, Nanoscale memristor device as synapse in neuromorphic systems. Nano Lett. 10(4), 1297-301 (2010). https://doi.org/10.1021/nl904092h
- H. Yeon, P. Lin, C. Choi, S.H. Tan, Y. Park, D. Lee, J. Lee, F. Xu, B. Gao, H. Wu, H. Qian, Y. Nie, S. Kim, J. Kim, Alloying conducting channels for reliable neuromorphic computing. Nat. Nanotechnol. 15(7), 574–579 (2020). https://doi.org/10.1038/s41565-020-0694-5
- 100. S. Choi, S.H. Tan, Z. Li, Y. Kim, C. Choi, P.-Y. Chen, H. Yeon, S. Yu, J. Kim, SiGe epitaxial memory for neuromorphic computing with reproducible high performance based on engineered dislocations. Nat. Mater. 17(4), 335-340 (2018). https://doi.org/10.1038/s41563-017-0001-5
- 101. P. Blennow, A. Hagen, K.K. Hansen, L.R. Wallenberg, M. Mogensen, Defect and electrical transport properties of Nb-doped SrTiO3. Solid State Ion. 179(35-36), 2047-2058 (2008). https://doi.org/10.1016/j.ssi.2008.06.023
- 102. S.-H. Yoon, H. Kim, Effect of donor (Nb) concentration on the bulk electrical resistivity of Nb-doped barium titanate. J. Appl. Phys. 92(2), 1039-1047 (2002). https://doi.org/10.1063/1.1486049
- 103. X.T. Zhang, Q.X. Yu, Y.P. Yao, X.G. Li, Ultrafast resistive switching in SrTiO3: Nb single crystal. Appl. Phys. Lett. 97(22), 222117 (2010). https://doi.org/ 10.1063/1.3524216
- 104. B. Chae, J. Seol, J. Song, K. Baek, S. Oh, H. Hwang, C. Park, Nanometerscale phase transformation determines threshold and memory switching mechanism. Adv. Mater. 29(30), 1701752 (2017). https://doi.org/10.1002/ adma.201701752
- 105. A. Mannodi-Kanakkithodi, M..Y. Toriyama, F..G.. Sen, M..J.. Davis, R..F. Klie, M..K..Y. Chan, Machine-learned impurity level prediction for semiconductors: the example of Cd-based chalcogenides. NPJ Comput. Mater. 6(1), 39 (2020). https://doi.org/10.1038/s41524-020-0296-7
- 106. A. Mannodi-Kanakkithodi, X. Xiang, L. Jacoby, R. Biegaj, S.T. Dunham, D.R. Gamelin, M.K.Y. Chan, Universal machine learning framework for defect predictions in zinc blende semiconductors. Patterns 3(3), 100450 (2022). https://doi.org/10.1016/j.patter.2022.100450

Springer Nature or its licensor holds exclusive rights to this article under a publishing agreement with the author(s) or other rightsholder(s); author self-archiving of the accepted manuscript version of this article is solely governed by the terms of such publishing agreement and applicable law.

Journal: 43579 Article: 243

## **Author Query Form**

# Please ensure you fill out your response to the queries raised below and return this form along with your corrections

#### Dear Author

During the process of typesetting your article, the following queries have arisen. Please check your typeset proof carefully against the queries listed below and mark the necessary changes either directly on the proof/online grid or in the 'Author's response' area provided below

Query	Details Required	Author's Response
AQ1	As References [29,67] and [65,82] are same, we have deleted the duplicate reference and renumbered accordingly. Please check and confirm.	

Journal: Large 43579 Article No: 243 Pages: 1 MS Code: 243 Dispatch:	ch : 26-8-2022	-8-2022
--	----------------	---------